ELSEVIER

Journal of Wind Engineering
and Industrial Aerodynamics 93 (2005) 1–30

JOURNAL OF wind engineering AND industrial aerodynamics

www.elsevier.com/locate/jweia

The UWO contribution to the NIST aerodynamic database for wind loads on low buildings: Part 1. Archiving format and basic aerodynamic data

T.C.E. Ho*, D. Surry, D. Morrish, G.A. Kopp

Alan G. Davenport Wind Engineering Group, Boundary Layer Wind Tunnel Laboratory, University of Western Ontario, London Ont. Canada N6A 5B9

Received 20 November 2002; accepted 7 July 2004

Abstract

Wind tunnel testing of generic low building models has been carried out at the University of Western Ontario (UWO) in support of an initiative by Texas Tech University (TTU) and the United States National Institute of Standards and Technology (NIST) to create an aerodynamic database for low building design. This paper describes the background of the project, the basic models, testing configurations, the wind simulation, the standard archival format for distribution of the data, and a basic analysis of the data. Part 2 presents a detailed comparison of the data with existing wind load provisions in building codes.

Basic quality checks of the data are made via limited comparisons among the data obtained during this study. Parametric comparisons based on roof slope, building height and building plan dimension show that the data obtained within this study are consistent with the expected aerodynamic behaviour. Comparisons with full scale TTU data show that the wind tunnel tests match the full-scale reasonably well, but cannot reproduce the largest of the peak point suctions near roof edges.

Keywords: Low buildings; Wind loads; Building codes; Aerodynamic database

*Corresponding author. Tel.: +1-519-661-3338; fax: +1-519-661-3339.
E-mail address: ericho@blwtl.uwo.ca (T.C.E. Ho).

0167-6105/$ - see front matter © 2004 Published by Elsevier Ltd.
doi:10.1016/j.jweia.2004.07.006

1. Introduction

The current North American provisions for wind loads on low buildings (e.g., [1–3]) are based largely on wind tunnel experiments conducted at the University of Western Ontario in the late 1970s [4]. Until recently, the data set was still the most comprehensive collection of wind load information on low buildings. Limited by the state of the technology at the time, there was no opportunity for post analysis of the wind tunnel data as the bulk of the data was discarded in favour of the measured statistical quantities of both local peaks, and structural load effects calculated on-line using a selection of influence coefficients. The measured peaks were condensed for codification. The codified structural load specifications were developed through assumed critical load effects on a number of typical structural systems, although the distributed load shapes were not sensitive to the details of the structural system. The load provisions were derived by enveloping the data sets for a number of parameters such as height, roof slope, size and other building features such as parapets. Also, the variation due to model scale was investigated but was not part of the codification process; the codified values were largely based on the 1:250 scale model tests, since the results were found to be relatively insensitive to scale.

There is now a much better understanding of low building aerodynamics and the techniques for model scale simulation. Recent full-scale experiments carried out at Texas Tech University (TTU) have set a widely accepted benchmark. They have largely confirmed model experiments except for local pressures very close to corners where some deficiencies in the ability of model testing to reproduce full-scale phenomena have been observed. Even though there is evidence that engineered buildings based on the current codes have had good safety records in high winds, a few questions remain whether these model scale deficiencies affect the design of buildings.

There is now also improved technology in terms of instrumentation and computer storage as well as access to public domain information through the Internet. Improved computing capability allows the use of detailed time histories of wind loads to be applied to a computer-simulated building structure for determining dynamic responses. These developments point to the possibility of designing low buildings dynamically using structural analysis programs with dynamic wind load data.

As part of the "NIST/TTU Cooperative Agreement—Windstorm Mitigation Initiative", a testing program was initiated by Dr. Emil Simiu of National Institute of Standards and Technology (NIST) to create a low building database for the purpose of providing time series of wind load data for public access for use in the design of low buildings. The idea has been summarized in Simiu and Stathopoulos [5], Whalen et al. [6] and Rigato et al. [7]. A building designer will be able to pick up, through public access, aerodynamic and climatological data that are appropriate for the building being designed.

An earlier test program directed by NIST was carried out at UWO in 1997 on a single generic low building model [8]. The test program provided simultaneously measured wind pressure data that have been used to demonstrate the application of

database assisted design [6,7]. Tests were carried out on a 1:200 model in open and suburban exposures. The same 1:200 simulation of the suburban exposure was used to test a 1:100 building model, thus creating a mismatch of the turbulence intensities and scales. Turbulence intensities for the 1:100 open exposure simulation were also too high. As part of the current program, the 1:200 model used in the 1997 NIST tests was upgraded to provide full coverage of pressure taps on all building surfaces and was tested in simulated 1:200 open and suburban exposures. The same model was also tested in simulated 1:100 open and suburban exposures. Other parameters studied include the effects of building length and parapets. This portion of the data set is not reported herein.

As part of the database development, the generic building models have been made available to be tested in other laboratories. The wind tunnel data from these different facilities will be compared for the assessment of the reliability of the testing facilities and procedures. At the beginning of this current program, wind tunnel testing of the models of the TTU full-scale test building has been carried out at three different laboratories. These results will be compared with results from the full-scale experiments in a future paper (with some limited comparisons presented here). With these benchmarks, a consensus on the standard of quality will be developed. Other testing facilities are welcome to participate in the development of the database once the quality of the testing facility is judged acceptable.

With the almost limitless possibilities of building geometries for low buildings, the database will rarely have the exact building geometry that a designer needs. This necessitates development of interpolation techniques or guidelines for choosing appropriate data sets for use. Research along this line is on-going at UWO and is reported elsewhere [9–12].

The dissemination of the aerodynamic database is a crucial component of the project in order for the data to be most useful. In the past, the dissemination of scientific data has been through published papers or reports that have often been in summary form. The bulk of the data are often unavailable. Even if they were provided in detailed reports, hard copy versions of pressure or load data would be very difficult to use. Typically, the only form of data availability has been through direct contact with laboratories. Additional problems arise when the person originally responsible for the data is no longer available, for whatever reasons, or the data format or storage media have become outdated. More efficient methods of data dissemination have been made possible by the popular use of the Internet; particularly its broadband data transfer capability and the use of reliable, large capacity digital media such as digital versatile discs (DVD). A consistent archival format is required such that the data are accompanied by the detailed model information and testing characteristics so that there is no ambiguity in the interpretation of the data.

The objective of the present paper is to provide a summary of the UWO contribution to the database with a particular focus on the archival format, the testing parameters, a limited discussion on the variation of the surface pressures with these parameters, and a comparison of measured pressures with some available full-scale data. Because of the ultimate use of the data reported herein by many different

users, the authors have included information that is important to the interpretation and use of the data that may not normally appear in such a paper. A summary of the wind tunnel data, in the form of structural loads is reported in the companion paper [13].

2. The wind tunnel models

2.1. Building Geometry

Seven building models were tested in the Boundary Layer Wind Tunnel II at UWO. These include four models of the same plan dimensions, 38.1 m × 24.4 m, (125 ft × 80 ft) for four roof slopes ($\frac{1}{4}$:12, 1:12, 3:12 and 6:12) for a range of eave heights between 3.66 m (12 ft) and 12.19 m (40 ft), and three more models with different plan dimensions of 19.1 m × 12.2 m (62.5 ft × 40 ft), 76.2 m × 48.8 m (250 ft × 160 ft) and 57.2 m × 36.6 m (187.5 ft × 120 ft), with 1:12 roof slope and with the same height range. The last three models were tested in order to investigate the effects of building size. All models have a length scale of 1:100.

All models were built and instrumented for the tallest 12.19 m (40 ft) building. Height adjustment for the model is achieved by sliding the model through a base plate with an opening of the same size as the building exterior dimensions. Table 1 summarizes the model configurations tested while Fig. 1 shows the 1:12 roof slope, 12.19 m (40 ft) building model as an example. The rectangular and circular openings seen on the long face of the model in the photograph were used in different dominant opening configurations for internal pressure measurements. (Details of internal pressure measurements are discussed below.)

2.2. Pressure tap layout

All models have the same layout of about 300 pressure taps on the roof, based on vertical projection. The exception to this is for the taps around the edges of the roof where they are at a nominal distance of 152 mm (6 in), equivalent full-scale, from the edge for all building models. Fig. 2 shows the exploded view of the pressure tap layout on the 1:12 roof slope building. The side walls also have the same layout. The pressure taps on the gable ends are slightly different near the gable peak. Figs. 3 and 4 show the pressure tap layouts of the gable end walls and the side walls for the $\frac{1}{4}$:12, 3:12 and 6:12 roof slope buildings, respectively. The layout of the pressure taps on the 19.1 m × 12.2 m (62.5 ft × 40 ft) and 38.1 m × 24.4 m (125 ft × 80 ft) building models are similar to the 1:12 roof slope model shown here.

2.3. Internal pressures

For the 1:12 roof slope, 38.1 m × 24.4 m (125 ft × 80 ft) building, internal pressure measurements were taken for three opening cases; namely, distributed leakage, a

Table 1
Wind tunnel model parameters

Roof slope	$\frac{1}{4}$:12	1:12	3:12	6:12	1:12	1:12	1:12
Plan dimension	38.1 m × 24.4 m (125′ × 80′)	38.1 m × 24.4 m (125′ × 80′)	38.1 m × 24.4 m (125′ × 80′)	38.1 m × 24.4 m (125′ × 80′)	19.1 m × 12.9 m (62.5′ × 40′)	76.2 m × 48.8 m (250′ × 160′)	57.2 m × 36.6 m (187.5′ × 120′)
Building height	3.66 m, 5.49 m, 7.32 m, 9.75 m, 12.19 m (12′, 18′, 24′, 32′, 40′)	4.88 m, 7.32 m, 9.75 m, 12.19 m (16′, 24′, 32′, 40′)	4.88 m, 7.32 m, 9.75 m, 12.19 m (16′, 24′, 32′, 40′)	3.66 m, 5.49 m, 7.32 m, 12.19 m (12′, 18′, 24′, 40′)	3.66 m, 5.49 m, 7.32 m 12.19 m (12′, 18′, 24′, 40′)	3.66 m, 5.49 m, 7.32 m 12.19 m (12′, 18′, 24′, 40′)	3.66 m, 4.88 m, 5.49 m 7.32 m 12.19 m (12′, 16′, 18′, 24′, 40′)
Opening configurations for internal pressures	Distributed leakage	Distributed leakage, small opening,[a] large opening[a]	Distributed leakage	Distributed leakage	Distributed leakage	Internal pressure not measured	Internal pressure not measured
Number of taps	659 external, 3 internal	665 external, 2 internal	677 external, 2 internal	701 external, 3 internal	665 external, 3 internal	665 external	694 external

[a]For 4.88 m (16′) and 12.19 m (40′) building heights only.

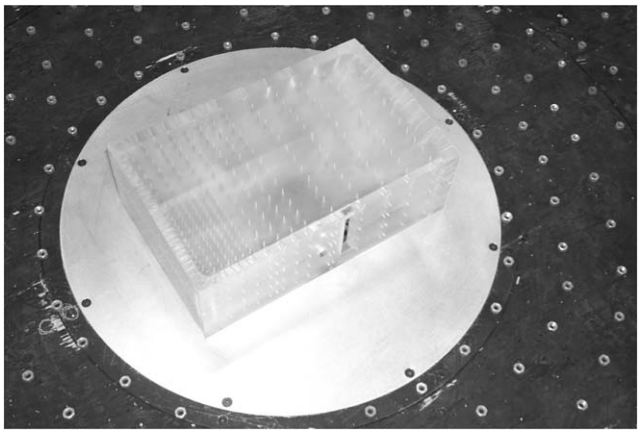

Fig. 1. Close-up photograph of one of the building models in the wind tunnel.

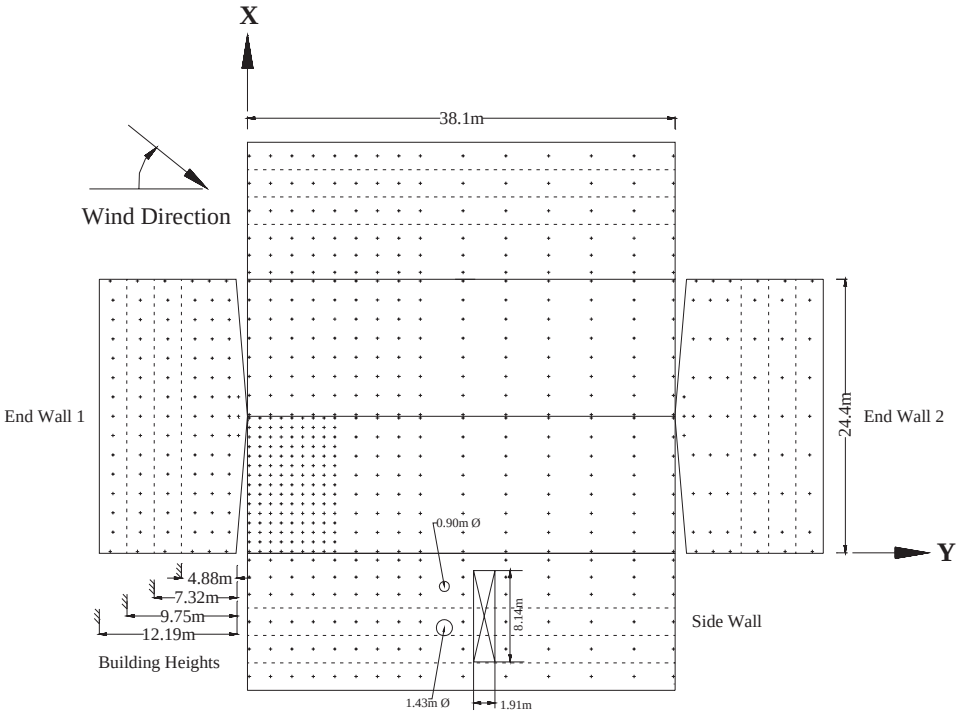

Fig. 2. Exploded view of the 38.1 x 24.4 m^2 building with a roof slope of 1:12. The pressure taps are indicated by the symbol, +.

small opening and a large opening (both with the background leakage open). In the case of dominant openings, internal pressures will be dynamic and this necessitates the modelling of the internal volume based on the dynamic response of the volume of

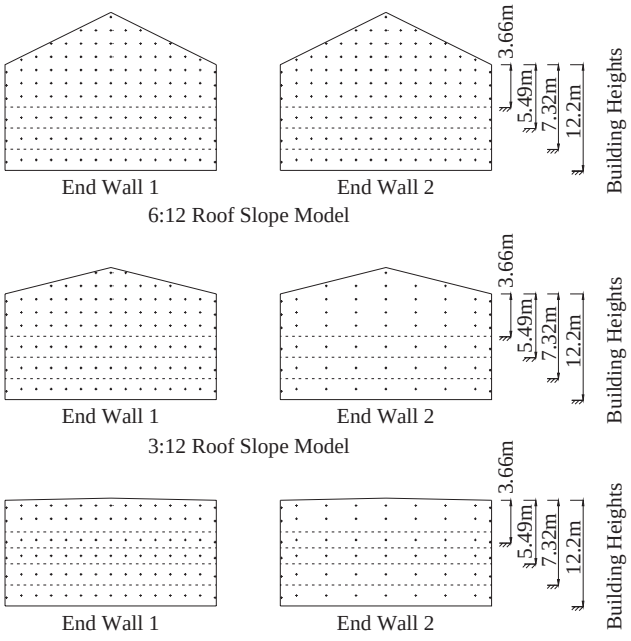

Fig. 3. Pressure taps on the gable end walls of the 6:12, 3:12 and $\frac{1}{4}$:12 roof slope buildings.

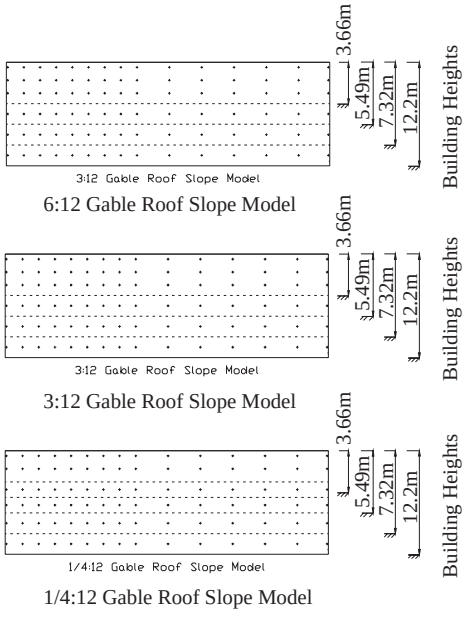

Fig. 4. Pressure taps on the side walls of the 6:12, 3:12 and $\frac{1}{4}$:12 roof slope buildings.

air as a Helmholtz resonator [14,15]. The modelling requirement is

$$\lambda_{\mathrm{vol}} = \frac{\lambda_{\mathrm{L}}^3}{\lambda_{\mathrm{vel}}^2},$$

where λ_{vol}, λ_{L} and λ_{vel} are volumetric, length and velocity scales, respectively. Upon satisfying the length scale requirement, the modelling requirement translates into a distortion of the internal volume of the model building by the square of the velocity scale.

A sealed volume chamber was attached to the bottom of the building model for tests with internal pressure measurements. For the case with dominant openings, the total internal model volume was approximately 0.18 m^3 (6.3 ft^3) corresponding to a scaled internal volume for the 12.19 m (40 ft) high building of about 11,800 m^3 (417,000 ft^3) with a velocity scale of about 1:4. For the 4.88 m (16 ft) buildings, a portion of the volume in the chamber was filled with Styrofoam in order to maintain the volume similitude.

The case of a small opening for the 4.88 m (16 ft) and 12.19 m (40 ft) building heights was represented by two circular openings with diameters of 8.97 mm (0.353 in) and 14.3 mm (0.563 in), in model scale, respectively. During the tests, the appropriate circular opening was left open while the other one was covered by tape. This provides a single small opening with the same total size as the distributed leakage of 0.1% of the total wall areas. For the case of a large opening, a rectangular opening of 81.3 mm × 19.1 mm (3.2 in × 0.75 in), in model scale, was put in the model for the case of the 12.19 m (40 ft) building. The opening was covered either entirely for the cases of distributed leakage and the small opening, or partially (for an opening of 33.3 mm × 19.1 mm (1.31 in × 0.75 in)) for the case of the 4.88 m (16 ft) building. The large opening has an area of 1% of the total wall area.

For the distributed leakage case, a series of 1.6 mm (1/16 in) diameter holes were put on the building walls to create a total leakage area of 0.1% of the total wall area. A total of 80 holes were distributed on four walls of the 38.1 m × 24.4 m (125 ft × 80 ft) building models. When the building height is reduced, the same proportion of number of holes were sealed and lowered beneath the wind tunnel floor, maintaining the ratio of total leakage areas for all building heights.

For most of the buildings tested, only internal pressures due to distributed leakage were measured (see Table 1). With only distributed leakage, the internal pressures are not expected to be highly dynamic; however, the volume chamber designed for the 1:12 roof slope building was installed for all those tests. The volumetric scaling for the 1:12 roof slope, 38.1 m × 24.4 m (125 ft × 80 ft) building with heights of 4.88 m (16 ft) and 12.19 m (40 ft) was maintained for the distributed leakage case but was not strictly maintained for other test cases.

2.4. Tubing system

A 762 mm (30 in) long tubing system was used to connect the pressure taps to solid state high speed pressure scanners. This tubing consists of a 305 mm (12 in) long PVC

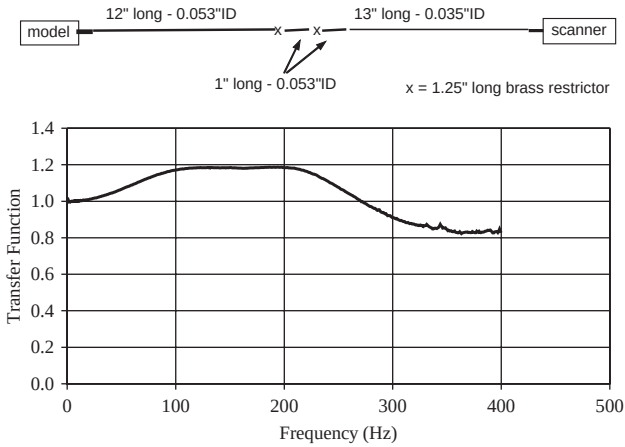

Fig. 5. Frequency response characteristics of the pressure tubing system.

tube with internal diameter of 1.35 mm (0.053 in) connected to the model which is connected by a pass-through plate with a 31.8 mm (1.25 in) long brass tubing going into the sealed chamber, two restrictors and a 330 mm (13 in) long PVC tube with internal diameter of 0.9 mm (0.035 in) connecting to the pressure scanner. The frequency response of this tubing system was tested in a separate testing chamber by measuring the transfer function of an input white noise signal and the signal after passing through the tubing system. Fig. 5 shows the tubing response with an illustrative diagram of the tubing arrangement used.

3. Wind simulation

The generic model tests include two homogeneous upstream terrain conditions; namely, open and suburban exposures. There is a wide range of definition for these typical exposures. Building codes define these conditions ranging from roughness lengths, z_0, between 0.01 and 0.15 m for open exposure and between 0.15 and 0.7 m for suburban exposure. Although power law wind profiles are widely used in building code formulation, they do not have a consistent complementary definition for turbulence intensities. Basic z_0 values of 0.03 and 0.3 m have been chosen for the definition of open and suburban exposures, respectively. The wind speed and turbulence intensity profiles and the spectral densities for the appropriate roughness lengths have been determined from the ESDU documents [16–18] and have been used as the benchmark for the wind simulation in the wind tunnel. These earlier ESDU documents have been chosen as benchmark for the spectra, since the turbulence scales are more realistic.

All the current set of wind tunnel tests were carried out in the Boundary Layer Wind Tunnel II at UWO. The high-speed test section of this wind tunnel has a cross

section of 3.4 m (11 ft) wide and a variable height between 1.8 m (6 ft) and 2.7 m (9 ft). The length of the upstream fetch to the centre of the turntable is about 30 m (100 ft). The tunnel floor is lined with automatic roughness elements, which are pneumatically controlled metal blocks that can be raised up to 200 mm (8 in) above the tunnel floor. Without additional devices, this wind tunnel can naturally generate homogenous wind characteristics at a length scale of about 1:400–1:500. For the current set of tests, additional turbulence generating devices, including three 1.5 m (5 ft) tall spires and a 380 mm (15 in) tall barrier across the wind tunnel at the entrance were added. These create turbulence characteristics consistent with a length scale of about 1:100. Fig. 6 shows the arrangement of the spires and the barrier at the entrance of the wind tunnel section.

Various heights of roughness elements were used along the wind tunnel floor to provide mixing of the wind gusts and generate the boundary layer characteristics. The heights of the roughness blocks were calibrated to create wind speed and turbulence intensity profiles matching that of the ESDU benchmarks. Note that the required roughness blocks tend to be relatively higher for the model case than in full scale. For this reason, it is unrealistic to continue these roughness elements right up to the model. In addition to the roughness blocks up to about 1.8 m (6 ft) upstream of the center of the turntable where the model is located, machine nuts (for 5/16 in screws) were scattered approximately 75 mm apart in the area between the roughness blocks and the model to sustain the turbulence intensities at the lowest heights for the incident winds. Figs. 7 and 8 show the mean wind speed and turbulence intensity profiles for the open and suburban exposures, respectively, compared with the ESDU profiles. In practice, since the pressure coefficients are eventually normalized by the roof height mean dynamic pressure, it is the match between turbulence intensities that is considered most important [19]. The agreement between the target and model scale profiles is good, except for the mean wind speed below 10–15 m in

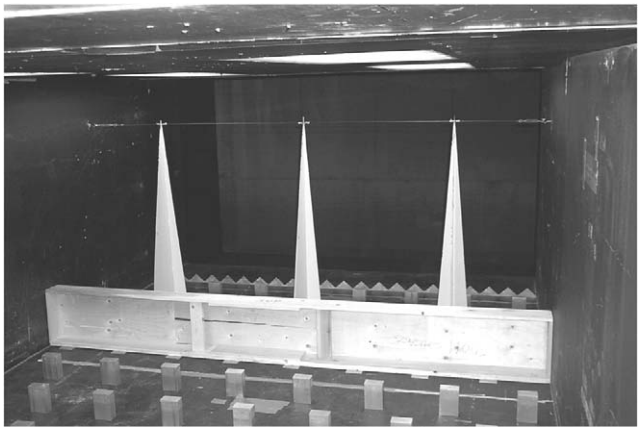

Fig. 6. Photograph of the turbulence generating devices near the entrance to the wind tunnel test section (looking upstream).

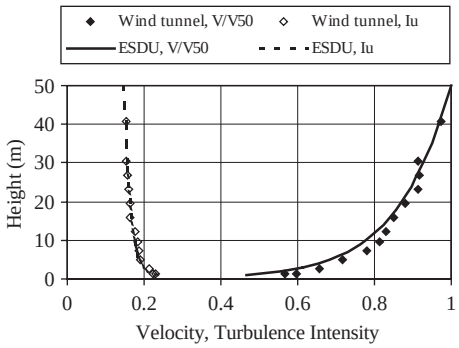

Fig. 7. Mean wind speed and turbulence intensity profiles in the open exposure.

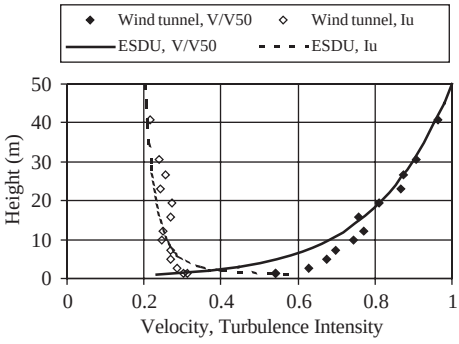

Fig. 8. Mean wind speed and turbulence intensity profiles in the suburban exposure.

the suburban exposure. This was difficult to match in the wind tunnel, but it should be kept in mind that this difference is less obvious when matched at any of the roof heights (and the turbulence intensities match well), in which case it is the flow above the roof where the mismatch actually occurs.

Figs. 9 to 11 show the longitudinal, lateral and vertical wind spectra at 10 m (32 ft) for open exposure. The figures show a mismatch of the longitudinal turbulence scale by about a factor of two based on the shift in the high frequency end of the spectra. Effects of a mismatch in turbulence length scale have been discussed in previous work [20,21]. This level of mismatch is likely to be inconsequential for point pressures and averages over small areas where the pressure patterns are dominated by the eaves height and local corner geometry that generate the flow separations, as shown by Lin and Surry [22]. The scale mismatch would be expected to have more importance for area or frame loads where the spatial correlation of the loads are important; however, even here a factor of two in scale is moderated dramatically when translated into an area integral (see Surry [21] for example). Typically, the order of error associated with a scale mismatch of a factor of two should be in the 5–10% range.

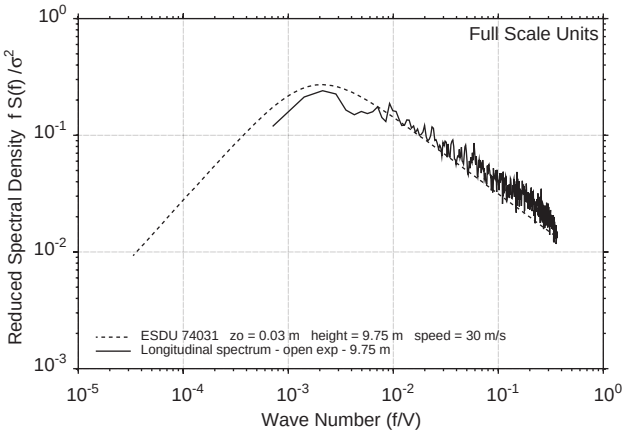

Fig. 9. Longitudinal wind spectrum at 9.75 m (32 ft) above ground in the open exposure.

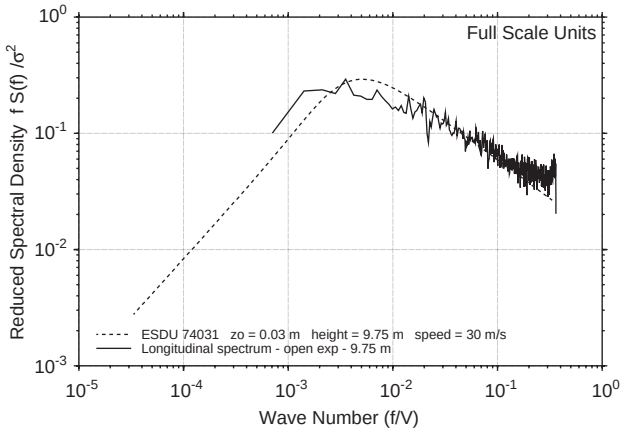

Fig. 10. Lateral wind spectrum at 9.75 m (32 ft) above ground in the open exposure.

4. Wind tunnel measurements

A high speed solid state pressure scanning system was used to take the pressure measurements. Measurements were taken at 37 wind angles over a 180° range at 5° increments (see Fig. 2 for the definition of wind angles). For the 1:12 and 3:12 roof slope building tests, measurements were taken between 180° and 360° except for the 57.2 m × 36.6 m (187.5 ft × 120 ft) building. For that building and for the $\frac{1}{4}$:12 and 6:12 roof slope buildings, measurements were taken between 270°, through 0°, to 90°. The highest density of pressure taps is windward for the cornering wind at about 315° in all cases.

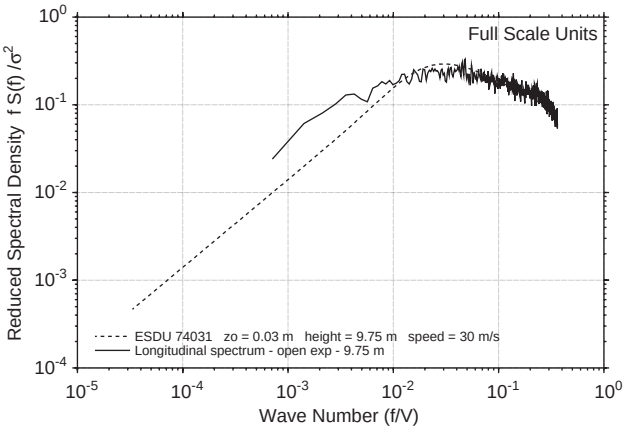

Fig. 11. Vertical wind spectrum at 9.75 m (32 ft) above ground in the open exposure.

Table 2
Measurement configurations and parameters

Model scale	1:100
Sampling frequency	500 Hz
Sampling period	100 s
Test angles	Every 5° over a 180° range (see Fig. 2 for definition of wind angles)
Upstream exposures	Open and suburban
Nominal wind tunnel speed at reference height	13.7 m/s (45 ft/s)

All instrumented taps were measured essentially simultaneously. The measurements taken within the sampling cycle have a maximum time lag of 15/16 of the sampling rate. In this case, the maximum time lag is approximately $15/16 \times 0.002$ seconds = 1.875 ms. The time lag is corrected by linear interpolation of the data within the same sample cycle.

Table 2 summarizes the test parameters which are common for all tests. Pressure data were taken at 500 samples per second for 100 s. Based on a mean, full-scale wind speed at 10 m height of 84 mph, the sampled data are equivalent to about 22 samples per second for 0.64 h in full scale for the open exposure tests and equivalent to about 29 samples per second for 0.48 h in full scale for the suburban exposure tests. All of the samples were stored for analysis and for future distribution.

The peak (maximum and minimum) pressure coefficients reported herein have been Lieblein-fitted and hence are more statistically stable quantities than the measured peaks. This involves dividing the record into 10 parts, using the Lieblein BLUE formulation [23] with the 10 individual peaks used to estimate the mode and dispersion of the Type I extreme value distribution, and using these to obtain the "best" expected peak for the entire record.

5. Pressure coefficient re-referencing

It is widely accepted that aerodynamic data referenced to roof height dynamic pressure produce the least variability. All low building pressure data sets follow this convention, including those in building codes. It is also intended in this study that all acquired data will be presented and compared based on such a definition. However, all the time series files are stored referenced to the dynamic pressures taken at an upper level in the wind tunnel where the flow is uniform with low turbulence levels. This ensures accurate speed control of the wind tunnel and accurate calibration of the pressure scanners. Conversion factors, corresponding to the ratio of the roof height to reference height dynamic pressures are required to convert the aerodynamic data to roof height reference. The roof height referenced pressure coefficients are defined using the following expression: $C_{p_H} = P/q_H = (P/q_{\text{ref}})(q_{\text{ref}}/q_H)$, where P is the difference between the model surface pressure and the reference level static pressure, q_{ref} is the dynamic pressure at the reference height, $C_{p_{\text{ref}}} = P/q_{\text{ref}}$ is the measurement obtained from the wind tunnel experiments and $q_{\text{ref}}/q_H = (V_{\text{ref}}/V_H)^2$ is the ratio of the dynamic (velocity) pressure at the upper level reference height in the wind tunnel and the dynamic (velocity) pressure at roof height. These may be taken from the wind velocity profiles attached with the data set (see Section 6). Because of high turbulence near roof height, measurements taken at this level have significant uncertainty. For the current set of data, a number of separate measurements have been taken in order to arrive at a reasonable estimate of the factors. This is further discussed below.

Wind speed profile measurements have been taken for each of the terrain simulations. The measurements include hot-wires and Pitot-static tubes traversed to various heights above the wind tunnel floor. Two hot-wires were used, each travelling approximately half the height of the wind tunnel. Two Pitot-static tubes were mounted beside the hot-wires. While the hot-wires are capable of measuring mean wind speeds and turbulence intensities, they are sensitive to temperature changes, which must be accounted for. The Pitot-static tubes do not have the frequency response to give correct turbulence intensities and the mean velocities indicated in regions of high turbulence are uncertain because of errors in the measurement of static pressure in such a situation; rather, they are used as a cross-check of the mean wind speed at higher heights where turbulence intensities are moderate.

Because of the low height of the lowest buildings, the mean wind speed ratios at roof and reference height can be as small as 0.5. When converted to dynamic pressures, the ratio becomes 0.25 so that the conversion factor is in the order of 4. A small error in the wind speed ratio can affect significantly the pressure coefficients referenced to roof height.

In each series of the tests, dynamic pressures at the tallest roof height, i.e., 12.19 m (40 ft) equivalent full scale height, were directly measured. This reference measurement height was not changed for tests of lower roof heights since for lowest roof height cases a roof height Pitot-static tube located off the turntable can be affected significantly by the presence of the roughness elements. (Also, the high

turbulence intensities may introduce errors into the measured mean dynamic pressure as indicated above). To ensure repeatable measurements, intermediate height references (at 48.8 m (160 ft) equivalent full scale) using additional Pitot-static tubes upstream of the turntable at about the $\frac{1}{4}$ point of the width of the wind tunnel and at the centerline of the wind tunnel were installed and sampled in every test. These data are used based on the premise that the intermediate height measurements will give a reference related to upper level wind speed measurements during the time of the tests and hence serve as an overall monitor of the simulation.

In addition to the measurements taken during the tests, subsequent reference pressure measurements were taken and, although the data are variable, they showed consistency. However, they did not match the roof height measurements taken during the 1:12 roof slope, 38.1 m × 24.4 m (125 ft × 80 ft) building model tests. It was subsequently discovered that the 1:12 roof slope building model tests suffered from a static pressure problem where the reference static pressure leaked to ambient pressure instead of static pressure in the wind tunnel section. The bias of the static reference pressure was in the order of $C_p \approx -0.15$. Since the static pressure is the base pressure for both the reference dynamic pressure and the dynamic pressures measured on the model, it creates significant bias for small pressures while the large magnitude pressures are basically unaffected. With an approximate correction to that problem, all reference pressure/wind speed measurements are now consistent. All pressure data for the 1:12 roof slope 38.1 m × 24.4 m (125 ft × 80 ft) building model were re-measured in a separate test.

Table 3 summarizes the measurements of the ratio of the roof height wind speed (V_H), the intermediate height wind speed (V_{int}) as well as the ratio of the intermediate height wind speed and the upper level reference wind speed (V_{ref}). With no obvious differences among the tests, averages of the ratios taken in different measurements were used as best estimates. The final conversion factors are summarized in Table 4. It is interesting to see that the possible range of uncertainty of dynamic pressures based on these "best" estimates is within about ±10% for the lowest building height.

6. Data archival system

The NIST aerodynamic database will be used by a large group of researchers for an extended period of time. Currently, UWO routinely saves all pressure readings for later "off-line" analysis. These files are written in a binary form and consist of a descriptive header followed by several thousand scans of "raw" integer counts from the Analog-to-Digital (A/D) converter. This technique generates a large quantity of data. For example, a 650-tap building yields a 40 MB file when sampled at 500 Hz for 60 s or over 1.3 GB for a typical test with 36 wind directions.

In the past, data files consisting of raw time series from UWO have been sent to other researchers written in a hexadecimal format for compactness and cross platform readability. Although it provided a usable way of conveying the data, details about test parameters, model and wind tunnel configuration, etc. were stored

Table 3
Reference wind speed information from pressure measurements

Exposure	Eave height	V_H/V_{int}				V_{int}/V_{ref}					
		Profile (pitot)	Pressure meas. 1	Pressure meas. 2	Average	Profile (pitot)	Pressure meas. 1	Pressure meas. 2	Pressure meas. during tests (1:12)	Pressure meas. during test (3:12)	Average
open	4.88 m (16 ft)	0.713	0.747	0.766	0.742	0.790	0.791	0.772	0.784	0.777	0.783
	7.32 m (24 ft)	0.782	0.787	0.814	0.794	0.790	0.779	0.779	0.784	0.775	0.781
	9.75 m (32 ft)	0.815	0.824	0.831	0.823	0.790	0.778	0.770	0.784	0.772	0.779
	12.19 m (40 ft)	0.828	0.841	0.860	0.843	0.790	0.775	0.773	0.784	0.771	0.779
	18.29 m (60 ft)		0.893	0.896	0.895	0.790	0.791	0.771			0.784
suburban	4.88 m (16 ft)	0.666		0.660	0.663	0.711		0.695	0.704	0.705	0.704
	7.32 m (24 ft)	0.685		0.695	0.690	0.711		0.699	0.704	0.711	0.706
	9.75 m (32 ft)	0.729		0.731	0.730	0.711		0.687	0.704	0.704	0.701
	12.19 m (40 ft)	0.766		0.748	0.757	0.711		0.701	0.704	0.704	0.705
	18.29 m (60 ft)			0.789	0.789	0.711		0.692			0.702

Table 4
Conversion factors for aerodynamic data from reference heights to roof heights

Exposure	Eave height	V_H/V_{ref}	q_{ref}/q_H
Open	3.66 m (12 ft)	0.561	3.18
	4.88 m (16 ft)	0.581	2.96
	5.49 m (18 ft)	0.587	2.90
	7.32 m (24 ft)	0.621	2.60
	9.75 m (32 ft)	0.641	2.43
	12.19 m (40 ft)	0.656	2.32
Suburban	3.66 m (12 ft)	0.447	5.00
	4.88 m (16 ft)	0.467	4.59
	5.49 m (18 ft)	0.468	4.57
	7.32 m (24 ft)	0.487	4.21
	9.75 m (32 ft)	0.512	3.82
	12.19 m (40 ft)	0.534	3.51

separately from the data. It became clear that as the number of data sets and configurations increases, the possibility of introducing errors due to miscommunication of experimental parameters increases.

The overall objective of the current archiving system is to provide the user with all the information needed to define the experiment within which the data were taken, and to allow the user to extract the data needed for further analysis. The information provided for the user includes pictures of the model and set-up, and whatever ancillary supporting information is deemed necessary to define the tests.

6.1. Selection of data format

Among several 'standard' data formats used within the scientific community, the (National Center For Supercomputing Applications) (NCSA) Hierarchical Data Format (HDF) was selected for the archive. This format was chosen for several reasons:

1. A large existing base (several platforms and languages) of public domain software libraries to access and manipulate HDF files;
2. The ability to manipulate large arrays and individual data items within a single container file; and
3. Continually improving support for HDF files in MATLAB which was the language chosen to develop the UWO supplied software.

Further details regarding the HDF format are available in [24]. The key features of format are given in the following sub-sections.

6.1.1. Self documentation

In order for the files to be self-documenting, a file-naming scheme which conveys information about the major test parameters, by encoding them into specific

fields of the filename, has been adopted. For example, the typical file name of *ADW100o100S048axxxx.HDF* provides information on the originating facility, the roof slope, the exposure, the model scale, the leakage case for internal pressures, the building eave height and the wind angle:

pos 1–3	identifies the originating facility:
pos 4–6	identifies the roof slope in 12ths to 3 digits
pos 7	identifies the exposure
pos 8–10	identifies the model scale to 3 digits
pos 11	identifies the leakage case
pos 12–14	is the building eave height in full scale feet to 3 digits
pos 15	is the index for different cases with otherwise the same filename
pos 16–19	is the wind angle in degrees to be read as xxx.x
.HDF	identifies the data format as a Hierarchical Data File

The file includes a header that contains all possible details for interpreting the data. Due to the size of data sets within the file, the headers can be relatively large and still make up a small percentage of the file. Some items within the comprehensive file header are:

- time stamp, the experiment's title, and originating laboratory
- azimuth, wind speed (roof height and reference height).
- file size: number of records times the size of records.
- wind profile information
  - o mean wind speed
  - o turbulence intensity
  - o spectral density function
- tap locations/ tap mapping within the file
- details of model geometry

The last three points are achieved by referencing external profile and drawing files.

6.1.2. Building geometry and tap locations

The HDF files contain data items with supporting information for the data set. For example, information on the order of the data, the tap number and the building face number on which the tap is located are provided. To complement the tap coordinate information, data items of the building geometry and the tap locations in 3D coordinates as well as in 2D coordinates of a flattened coordinate system are available to draw a wire frame outline of the building and the tap locations for illustration.

6.1.3. Data handling

The data handling routines supplied by the NCSA as part of the HDF standard have the ability to extract any slice of any data item within an HDF file. These routines have been incorporated into the MATLAB HDF support facility. Specific

functions have been developed to load and read the data set. Subroutines could be written to provide the casual user with data on a scan-by-scan basis thereby isolating the user from learning the mechanics of file buffers, etc.

6.2. Data generated at other facilities

For the archiving of data generated at other testing facilities, the MATLAB source code used for creating the UWO archives is available. This may be adapted by individual facilities to fit their raw data file format for conversion to the HDF file format. This program requires several basic input items to complete the documentation of the data set. The names of the required input files are assembled based on rules and information contained in control files which act as lookup tables.

7. Comparison of data within the database

The following comparisons provide an initial summary of the low building database by examining the spatial variation of the mean and rms pressure coefficients. The analysis makes use of all of the building configurations tested at UWO to separately examine the effects of roof slope, building height and building plan dimension on local pressure coefficients. This was repeated along two lines of pressure taps, firstly at mid-span (for a wind direction of 270°) and secondly at a short distance from the building edge (for a wind direction of 325°). Only the results from the open country terrain will be discussed.

7.1. Effects of building height

Comparisons were made to determine the effect of building height on wind loads. This was performed for the three variations of roof slope, although only the results from the 1:12 building are presented here. It is the current understanding for building roofs large enough for flow reattachment to take place that local pressure coefficients on the surface underneath the separated flow, when referenced to an eaves height dynamic pressure, e.g., q_H, are dependent on the ratio of $(x, y)/H$, or, distance from leading edge/building height Fig. 2 shows the coordinate system used for the roof area. The origin is at the building corner with the high tap density, with the x-axis in the direction of the gable end wall and the y-axis along the long side wall of the building. In particular, it is believed that once the flow has separated from the leading edge (or corner) of the building, the distance until the flow reattaches is proportional to the height of the building. This is shown in Fig. 12, which presents the spatial variation of the mean and rms pressure coefficients along the line of taps at mid-span, for a wind direction of 270°. Note that the distance from the tap to the leading edge of the building, x, is normalized by the eave height of the building, H. The figures show the pressure coefficients at the leading edge collapse reasonably well within the separated and reattached flow region for all buildings for $x/H < 1.0$. Deviations in the mean pressure coefficients begin to occur as the flow approaches

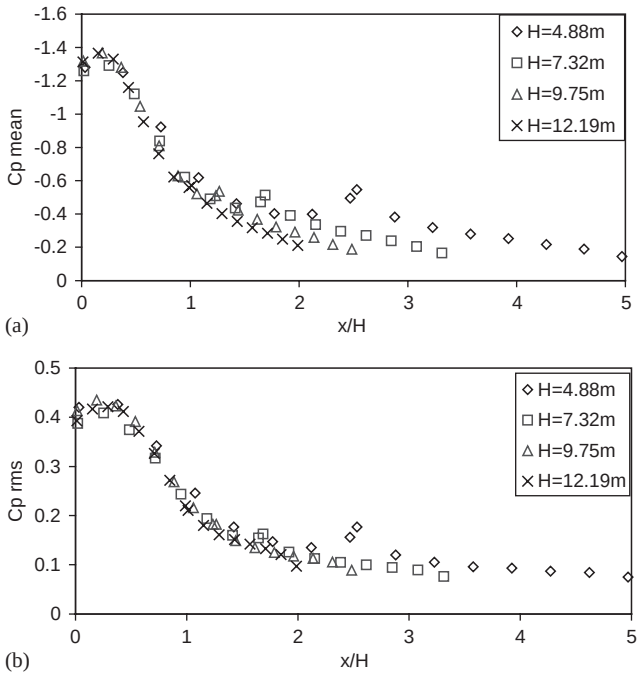

Fig. 12. Spatial variation of the (a) mean and (b) rms pressure coefficients along a line of taps at mid-span for buildings with a roof slope of 1:12 and for a wind angle 270°.

the building ridge, with secondary separation of the flow at the ridge of all four building heights. Since the plan dimensions are not geometrically similar with respect to H, the ridge appears at different x/H. It can be seen in Fig. 12(a) that the pressure levels off on the 4.88 m (16 ft) building prior to the ridge for $x/H > \sim 1.4$, indicating fully reattached flow. This is similar on the 7.32 m (24 ft) building. There is clear evidence of increases in mean and rms pressure coefficients at the ridge for the 4.88 m (16 ft) and 7.32 m (24 ft) buildings. Slight increases in mean pressure coefficients can also be seen at the ridge on the 9.75 m (32 ft) and 12.19 m (40 ft) buildings, indicating the flow is not in the same condition before reaching the ridge, at x/H of 1.25 and 1.0, respectively. At this point, it is not clear what kind of normalization could collapse the data in the lee of the ridge. Since the flow adjusts to the presence of the ridge upstream of the ridge, normalization based on the distance from the ridge, for locations in its lee may not be entirely appropriate. It should be noted that, over the complete roof, the neural network approach of Chen et al. [9] captures the variations of the mean and rms pressure coefficients more accurately than this simple relationship with roof height.

Similar comparisons were performed for a line of taps located a distance approximately $y/H = 0.41$ from the building edge and for a wind direction of 325°. These are presented in Fig. 13. In this case, the line of pressure taps is chosen such that it crosses the path of both corner vortices. Different rows of pressure taps were

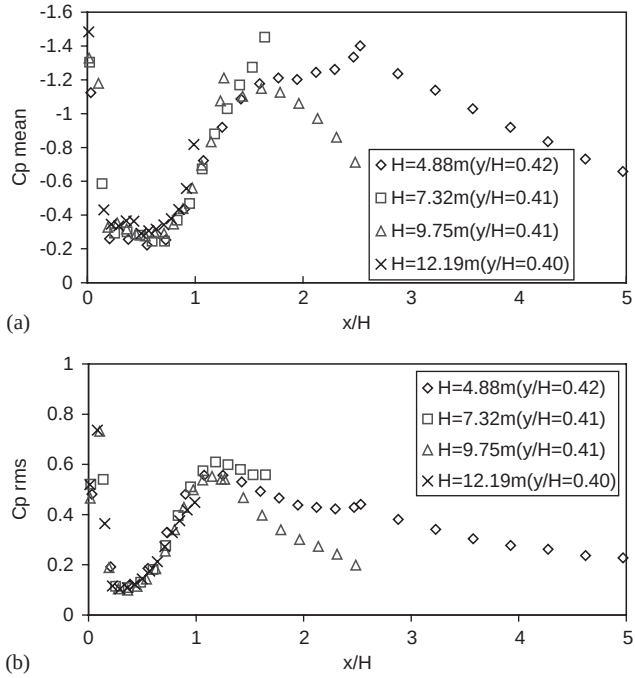

Fig. 13. Spatial variation of the (a) mean and (b) rms pressure coefficients along a line of taps near the edge of the building for a roof slope of 1:12 and a wind angle 325°.

used for different building heights in order to maintain similar ratios of y/H for comparison. As such, no pressure taps are available for comparison in the lee of the ridge for the 7.32 m (24 ft) and 12.19 m (40 ft) buildings. The distribution of the mean and rms coefficients clearly show the presence of the two corner vortices by the large rms values at the leading edge and again at $x/H \approx 1.2$. The figures indicate that $(x, y)/H$ is a reasonable normalizing parameter for the pressure distribution up to the flow in the lee of the first reattachment, consistent with the findings of Lin and Surry [22]. For this line of taps, both the mean and rms coefficients are strongly affected by the ridge where the pressure gradient is high just ahead of flow separation at the ridge.

7.2. *Effect of roof pitch*

Four different roof slopes have been tested ($\frac{1}{4}$:12 , 1:12, 3:12 and 6:12) for buildings with the same plan dimensions of 38.1 m × 24.4 m (125 ft × 80 ft). Comparisons of the effect of roof pitch on local pressure coefficients are limited here to the building height of 7.32 m (24 ft) for the three lower roof slopes of $\frac{1}{4}$:12, 1:12 and 3:12. Fig. 14 presents the effect of roof slope on the mean and rms pressure coefficients measured at mid-span, for a wind direction of 270°. The figures indicate that the pressure distributions on the $\frac{1}{4}$:12 and 1:12 roof sloped buildings are similar for this wind

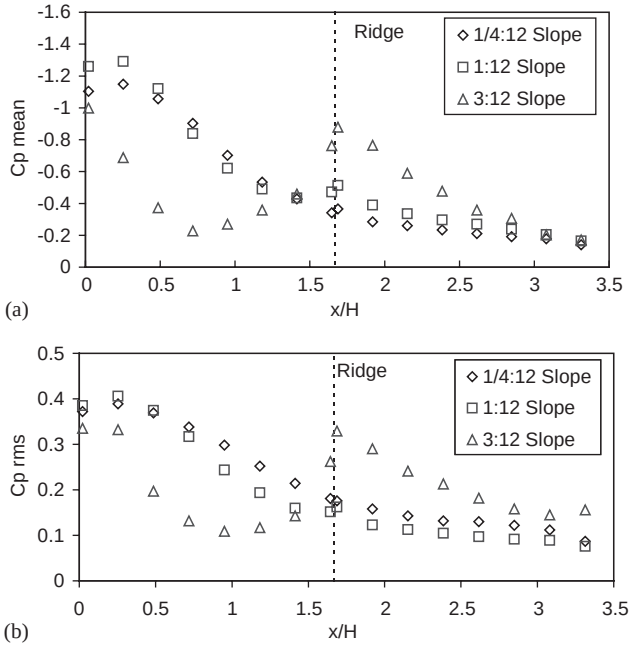

Fig. 14. Spatial variation of the (a) mean and (b) rms pressure coefficients along a line of taps at the midspan for buildings with different roof slopes and an eaves height of $H = 7.32$ m (24 ft) and for a wind angle of 270°.

direction, consistent with the assumption that roof slopes less than 10° have similar aerodynamic behaviour. Mean pressure coefficients for the 1:12 roof slope building are higher by about 10% at the leading edge and 30% behind the ridge. In absolute values, this equates to a difference in pressure coefficient of less than 0.15 in both instances. The results from the 3:12 roof slope indicate significant differences when compared to the other two slopes. As expected, the steeper roof slope leads to a significant reduction in suction pressures at the leading edge of the building because of the earlier reattachment; however, there is a significant increase in the suction pressures behind the ridge.

Similar trends were observed near the roof edge for winds approaching from 325°, as shown in Fig. 15, although the corner vortex appears to minimize some of the differences before the flow reaches the ridge. In this case, the third row of pressure taps was used for the comparisons ($y/H = 0.28$). Again, the $\frac{1}{4}$:12 and 1:12 buildings show similar pressure distributions until just before the ridge. Beyond the ridge, the mean and rms coefficients increase with roof slope.

7.3. *Effect of building plan dimensions*

All buildings tested in the current testing program have the same length to width ratio. For the 1:12 roof slope, four different building plan dimensions,

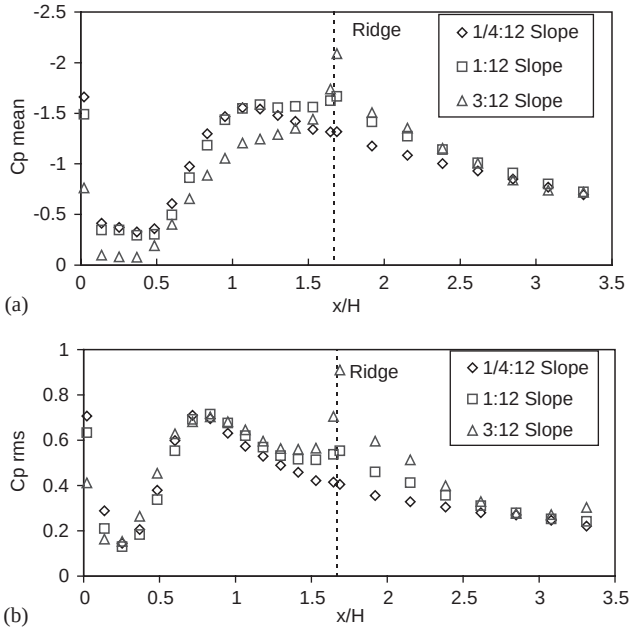

Fig. 15. Spatial variation of the (a) mean and (b) rms pressure coefficients along a line of taps at $y/H = 0.28$ for buildings with different roof slopes and an eaves height of $H = 7.32$ m (24 ft) and for a wind angle of 325°.

19.1 m × 12.19 m (62.5 ft × 40 ft), 38.1 m × 24.4 m (125 ft × 80 ft), 57.2 m × 36.6 m (187.5 ft × 120 ft) and 76.2 m × 48.8 m (250 ft × 160 ft), were tested. Among three of the buildings tested, appropriate roof heights are selected to compare buildings which are geometrically similar, i.e., 19.1 m × 12.19 m × 3.66 m (62.5 ft × 40 ft × 12 ft), 38.1 m × 24.4 m × 7.32 m (125 ft × 80 ft × 24 ft) and 76.2 m × 48.8 m × 12.19 m (250 ft × 160 ft × 40 ft—although this model has a slightly small eaves height. Fig. 16 presents the spatial variation of the mean and rms pressure coefficients recorded along the row of taps at mid-span for a wind direction of 270°, for each of the above buildings. Comparisons of the mean pressure distribution indicate a reasonable collapse of the data, given differences in the characteristics of the turbulence at the different eaves heights. The largest building size gives slightly higher mean pressures at the leading edge but otherwise all three buildings agree quite well. For rms pressures, Fig. 16(b) show good agreement among all three buildings except higher values for the smallest building at the leading edge.

8. Comparison with full scale TTU data

The previous comparisons show that normalized distance from the building edge, $(x, y)/H$, provides a reasonably good collapse of the aerodynamic data up to the first

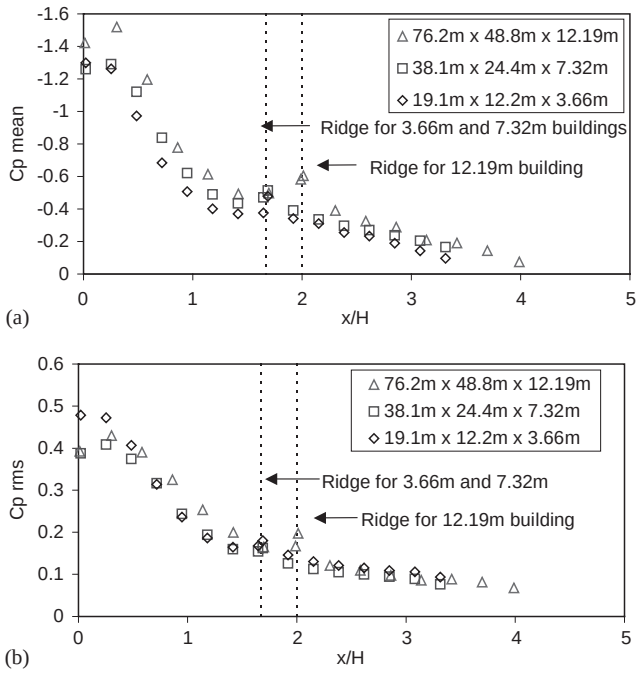

Fig. 16. Spatial variation of the (a) mean and (b) rms pressure coefficients along a line of taps at mid-span for (nearly) geometrically similar buildings with a roof slope of 1:12 and for a wind angle 270°.

reattachment for different building sizes. Comparison with the TTU field experiment data [25] will now be made to assess similar relationships with the full-scale data. It should be noted that the standard open exposure ($z_0 = 0.03$ m) used in the wind tunnel tests falls within the range of full scale terrain condition (10th and 90th percentile roughness length, z_0, of 0.01 m and 0.087 m, respectively) taken at TTU and the data are therefore generally comparable.

Fig. 17 shows mean, rms and peak pressure coefficients along the first row of pressure taps on the TTU building; i.e. taps 50101, 50501 and 50901. The TTU building has dimensions of 13.7 m × 9.1 m × 3.96 m (45 ft × 30 ft × 13 ft) with a $\frac{1}{4}$:12 roof slope. These are compared with the second row of taps on the $\frac{1}{4}$:12 roof slope, 38.1 m × 24.4 m × 12.19 m (125 ft × 80 ft × 40 ft), building tests, the equivalent y/H value is approximately 0.09. Data are available for the windward half of the roof up to $x/H = 1.0$. The comparison is for a cornering wind 325° from the long building axis. These included all data from the TTU experiments with wind directions within ±2.5°. They are compared to wind tunnel results at 325° (note that definition of wind angle is based on the convention of the current data). Fig. 17(a) shows that the mean pressures compare well. The rms pressure coefficients in Fig. 17(b) indicate significant differences although the trend is captured, with the wind tunnel data being lower. This is in line with previous model scale/full scale comparisons of the TTU Building [26,27]. Similar differences are observed in the peak pressure

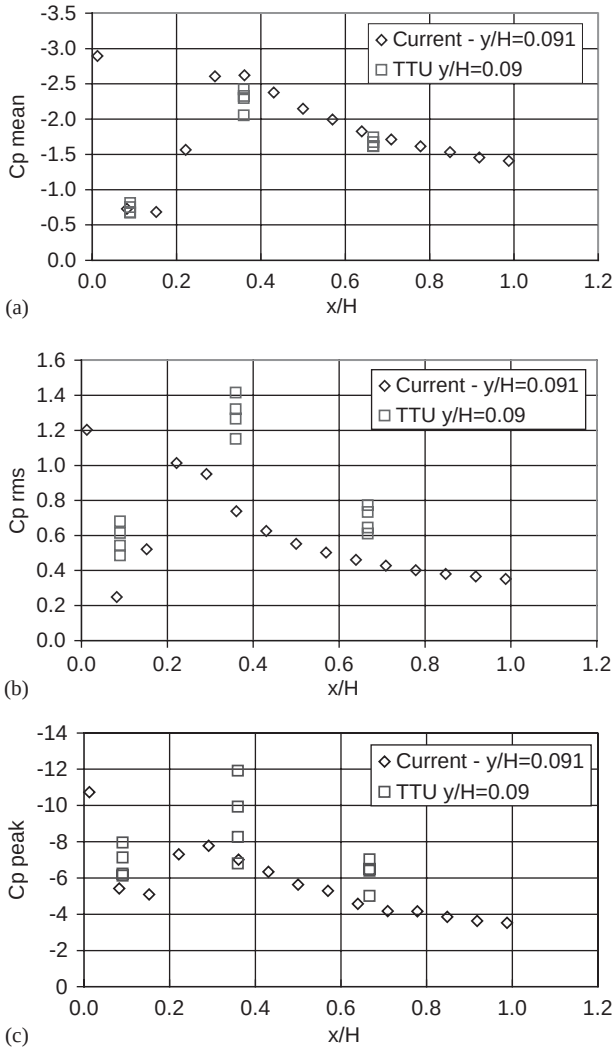

Fig. 17. Comparison of (a) mean, (b) rms, and (c) peak pressure coefficients from the current wind tunnel data with the TTU full scale data along a line near the leading edge for a wind angle of 325°.

coefficients shown in Fig. 17(c) where the negative peaks under the vortex at Tap 50501 are not reproduced in the wind tunnel tests. Near the edge of the building, the wind tunnel results show a large negative peak pressure coefficient of −10.7. The full scale data set does not have any pressure tap at this distance from the building edge. It is also interesting to observe that the wind tunnel data tends to envelope the lower range of the full-scale values.

Fig. 18 shows mean, rms and peak pressure coefficients versus wind angle for tap 50501 from the TTU full scale experiments and a comparable tap from the current

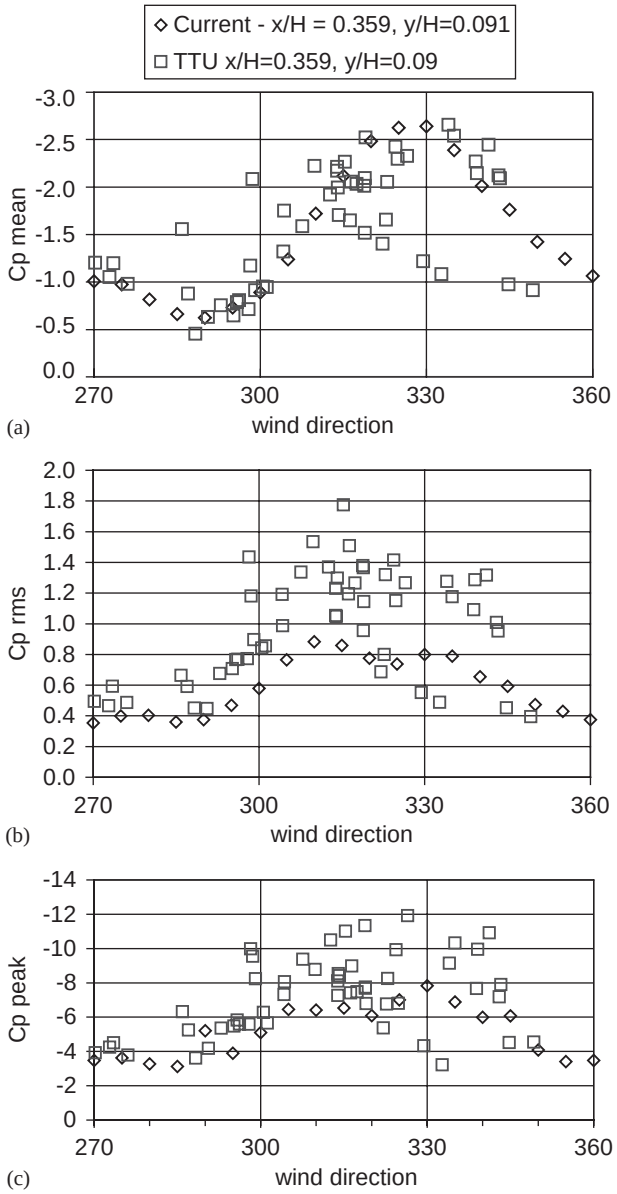

Fig. 18. Comparison of (a) mean, (b) rms, and (c) peak pressure coefficients from the current wind tunnel data with the TTU full scale data at a point near the leading edge.

NIST tests on the $\frac{1}{4}$:12 roof slope, 38.1 m × 24.2 m × 12.19 m (125 ft × 80 ft × 40 ft) building, based on normalized distance from the leading edge with $x/H = 0.36$ and $y/H = 0.09$. The comparison is limited to the cornering wind directions, equivalent

to the NIST test angle range of 270 °–360 °. Comparison of the mean pressure coefficients in Fig. 18(a) shows good agreement, given the large variability of the full scale data. The rms pressure coefficients shown in Fig. 10(b) from the current NIST data and the TTU do not match as well, although the wind tunnel data again envelope the lower range of the full-scale data. This is similar to previous comparisons carried out between the model tests of the TTU model and full-scale results [26–29]. Similar observations can be made for peak pressure coefficients from the current NIST test and the TTU full-scale data. It can be concluded that the wind tunnel technique used cannot reproduce the highest peaks obtained near the edges of the roof, but does seem to match the range of the lower end of the full-scale data.

9. Comparison with ASCE 7-02 recommended loads

The experimental results are compared with the existing American Society of Civil Engineers (ASCE 7-02) Standard [1], by comparing a number of area-averaged loading coefficients. The companion paper [13] presents a detailed comparison with wind load provisions for structural loads and also with Stathopoulos' data [4]. In addition to examining point pressure coefficients (single pressure taps), five area-averaged loading coefficients were developed at the leading corner of the building by simultaneously combining pressures recorded on a number of taps covering the area considered. The tap combinations used in the analysis are presented in Fig. 19, where

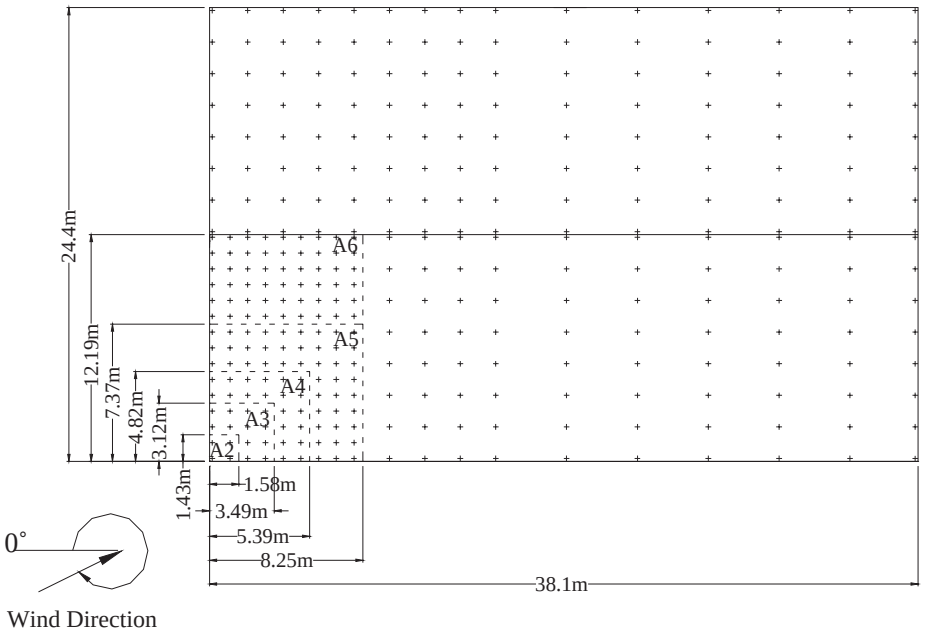

Fig. 19. Details of the areas and locations used in the area-averaging analysis.

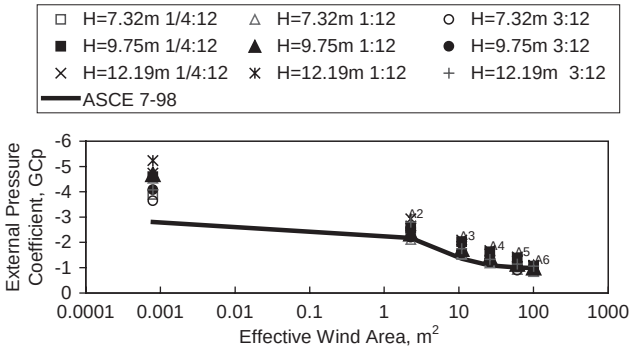

Fig. 20. Comparison of area-averaged coefficients GCp, with ASCE 7-02 coefficients.

the corner of each loading area corresponds to the corner point of the building. Note that these may not be the worst locations for each of these areas, especially the smaller ones.

Fig. 20 presents the minimum pressure coefficients versus loading area for a number of the current NIST data sets with constant plan dimensions of 38.1 m × 24.4 m (125 ft × 80 ft). The pressure coefficients presented in the figure represent the worst pressure coefficients recorded over all wind directions. Also included in the figure are the ASCE 7-02 recommended loading coefficients obtained for the corresponding loading areas, with all relevant reduction factors ignored in the analysis. All coefficients presented in the figure are normalized by the 10-m height, 3-second gust wind speed, as recommended by the ASCE 7-02 standard (see [13] for details).

The figure indicates that the area-averaged coefficients increase with building height, with the worst coefficients occurring on the lesser sloped buildings. The worst point pressure coefficient of –5.2 was recorded on the 12.19 m (40 ft) tall building with a 1:12 gable roof slope. In most cases the ASCE 7-02 derived loads were below the measured coefficients, in particular for the point pressures, where the $H = 12.19$ m (40 ft), 1:12 slope building configuration recorded a worst coefficient almost twice as large as the ASCE 7-02 derived load. However, the comparisons do improve for the larger areas, with the ASCE provisions underestimating the maximum experimental load by 30% for area ‘A2’ and by 20% for area ‘A3’.

10. Conclusions

The current data set represents the start of an extensive archive of low building aerodynamic data. With the participation of many more testing facilities, and improved technology to interpolate and extrapolate available data to other geometries, this program has the potential to become an extremely useful tool in low building design. The paper provides a brief examination of the current wind load database on low buildings obtained at UWO. The results are found to be consistent

among all data sets tested in the current testing program as indicated by the distribution of pressure coefficients normalized by distances from the roof edge, $(x, y)/H$. These are observed to collapse well for all buildings up to the first flow reattachment, except for areas near the ridge and for the steeper roof slope, as expected. In the comparison of the results, based on the normalized distance from the building edge, between the TTU full scale data and the $\frac{1}{4}$:12 roof slope building, it is found that the wind tunnel simulation cannot reproduce the larger rms and peak values for taps near the edges of the roof. This finding is consistent with earlier comparisons between full scale and model test results of the TTU building. It is encouraging that the wind tunnel simulation is able to envelope the lower range of the full-scale data, however. The comparison between the current data set and the ASCE 7-02 specifications suggests that the ASCE point pressure specifications may be lower, while the area loads match well for the lower eaves heights.

Acknowledgements

The funding for the experiments, and partial student support, was provided by NIST and TTU. NSERC (Canada) also provided student support. The ongoing support of Dr. Emil Simiu and Dr. Kishor Mehta is greatly appreciated. One of the authors (GAK) gratefully acknowledges the support of the Canada Research Chairs Program.

References

[1] American Society of Civil Engineers (ASCE), ASCE Standard, Minimum Design Loads for Buildings and Other Structures—ASCE 7-02, ASCE, Reston, VA, USA, 2002.
[2] Metal Building Manufacturers Association (MBMA), Metal Building Systems Manual, MBMA, Cleveland, OH, USA, 1996.
[3] National Research Council Canada (NRCC), The supplement to the National Building Code of Canada, NRCC, Ottawa, Canada, 1995.
[4] T. Stathopoulos, Turbulent Wind Action on Low-rise Buildings, Ph.D. Thesis, The University of Western Ontario, London, Ont., Canada, 1979.
[5] E. Simiu, T. Stathopoulos, Codification of wind loads on buildings using bluff body aerodynamics and climatological databases, J. Wind Eng. Ind. Aerodyn. 69–71 (1997) 497–506.
[6] T. Whalen, E. Simiu, G. Harris, J. Lin, D. Surry, The use of aerodynamic databases for the effective estimation of wind effects in main wind-force resisting systems:: applications to low buildings, J. Wind Eng. Ind. Aerodyn. 77–78 (1998) 669–685.
[7] A. Rigato, P. Chang, E. Simiu, Database-assisted design, standardization and wind direction effects, ASCE J Struct. Eng. 127 (2001) 855–860.
[8] J. Lin, D. Surry, Simultaneous time series of pressures on the envelope of two large low-rise buildings, Engineering Science Research Report BLWT-SS7-1997, Boundary Layer Wind Tunnel Laboratory, The University of Western Ontario, London, Ont. Canada, 1997.
[9] Y. Chen, G.A. Kopp, D. Surry, Prediction of pressure coefficients on roofs of low buildings using artificial neural networks, J Wind Eng. Ind. Aerodyn. 91 (2003) 423–441.
[10] Y. Chen, G.A. Kopp, D. Surry, Interpolation of pressure time series in an aerodynamic database for low buildings, J Wind Eng. Ind. Aerodyn. 91 (2003) 737–765.

[11] Y. Chen, G.A. Kopp, D. Surry, The use of linear stochastic estimation for the reduction of data in the NIST aerodynamic database, Wind and Struct. 6 (2003) 107–126.
[12] G.A. Kopp, G.A., Chen, Y. D. Surry, The NIST aerodynamic database for wind loads on low buildings: An expert system to expand the database, Proceedings of the 2003 ASCE/SEI Structures Congress and Exposition, Seattle, USA, CD-ROM, (2003).
[13] L.M. St. Pierre, G.A. Kopp, D. Surry, T.C.E. Ho, The UWO contribution to the NIST aerodynamic database for wind loads on low buildings: Part 2. Comparison of data with wind load provisions, J. Wind Eng. Ind. Aerodyn. 93 (2) (2005), in preparation.
[14] J.D. Holmes, Mean and fluctuating internal pressures induced by wind. Proceedings of the 5th International Conference on Wind Engineering, Colorado State University, Fort Collins, Colorado, 1979, pp. 435–450.
[15] B.J. Tryggvason, N. Isyumov, Similarity requirements for inflatable structures. Proceedings of the Third National Conference on Wind Engineering Research, Gainsville, FL, 1978, pp. 335–338.
[16] Engineering Science Data Unit (ESDU), Strong winds in the atmosphere boundary layer. Part 1: Mean-hourly wind speeds. Data Item 82026, 1982.
[17] Engineering Science Data Unit (ESDU), Strong winds in the atmosphere boundary layer. Part 2: Discrete gust speeds. Data Item 83045, 1983.
[18] Engineering Science Data Unit (ESDU), Characteristics of atmospheric turbulence near the ground. Data Item 74031, 1974.
[19] T.C.E. Ho, Variability of Low Building Wind Loads. Ph.D. Thesis. The University of Western Ontario, London, Ontario, Canada, 1992).
[20] T. Stathopoulos, D. Surry, Scale effects in wind tunnel testing of low buildings, J. Wind Eng. Ind. Aerodyn, 13 (1983) 313–326.
[21] D. Surry, Consequences of distortions in the flow including mismatching scales and intensities of turbulence, Wind Tunnel Modelling For Civil Engineering Applications, Cambridge University Press, Cambridge, 1982, pp. 137–185.
[22] J.X. Lin, D. Surry, The variation of peak loads with tributary area near corners on flat low building roofs, J. Wind Eng. Ind. Aerodyn, 77-78 (1998) 185–196.
[23] J. Lieblein, Efficient methods of extreme-value methodology, National Bureau of Standards, Washington, DC, Report No. NBSIR 74-602, 1974.
[24] http://hdf.ncsa.uiuc.edu.
[25] K.C. Mehta, M.L. Levitan, Field experiments for wind pressures. Department of Civil Engineering Progress Report, Texas Tech University, 1998.
[26] D. Surry, Pressure measurements on the Texas Tech Building: Wind tunnel measurements and comparisons with full scale, J. Wind Eng. Ind. Aerodyn. 38 (1991) 235–247.
[27] L.S. Cochran, J.E. Cermak, Full- and model-scale cladding pressures on the Texas Tech University experimental building, J. Wind Eng. Ind. Aerodyn. 41-44 (1992) 1589–1600.
[28] H. Okada, Y-C. Ha, Comparison of wind tunnel and full-scale pressure measurement tests on the Texas Tech Building, J. Wind Eng. Ind. Aerodyn. 41-44 (1992) 1601–1612.
[29] B. Bienkiewicz, H.J. Ham, A 1:50 scale wind-tunnel case study of wind pressure on TTU building, in: A. Larsen, G.L. Larose, F.M. Livesey (Eds.), Wind Engineering into the 21st Century Balkema, Rotterdam, 1999, pp. 1755–1762.